Learning-assisted mode selection for hybrid optical–acoustic underwater wireless communication under stochastic channel conditions

LENIN JOSEPH, SANGEETHA ANANDAN*
School of Electronics Engineering, Vellore Institute of Technology, Vellore, Tamil Nadu, India

Hybrid optical acoustic underwater wireless communication systems are a promising solution in meeting the challenges offered by complex underwater channels for reliable and efficient data transmission. This paper investigates learning assisted communication mode selection in hybrid optical acoustic underwater wireless networks under stochastic channel conditions, where machine learning classifiers are used to pre assess the link quality, followed by a Bayesian regularization neural network for refined mode selection and improved prediction under uncertain and diverse underwater conditions. Simulation results show better performance in terms of energy consumption, throughput, normalized mean traffic load, received load, and average power savings, compared to existing methods.

(Received March 17, 2026; accepted June 2, 2026)

Keywords: Underwater wireless communication, Hybrid optical acoustic networks, Mode selection, Bayesian regularization neural networks

1. Introduction

Dependable underwater wireless communication (UWC) is a major research question as it finds a lot of useful applications including marine and environmental monitoring, offshore infrastructure inspection, disaster prevention, autonomous underwater vehicle (AUV) communication and many other areas associated with the Internet of Underwater Things (IoUT) [1-2]. However, because of the challenges that occur in the underwater environment, such as high signal attenuation, multipath propagation, and limited bandwidth, realizing reliable and efficient UWC is still a major research problem. Because of its long transmission range, underwater acoustic communication (UAC) has historically been utilized among the available technologies; however, it has poor data rates and high latency. In contrast, water turbidity, scattering, and short transmission distances severely restrict the performance of underwater optical wireless communication (UOWC), which offers much higher data rates and lower latency. By combining the complementary strengths of both UAC and UOWC, hybrid optical–acoustic communication systems have emerged as a promising solution, as it overcomes the limitations of individual technologies. However, choosing the right communication mode effectively in a variety of underwater situations continues to be a significant challenge [3]. In this situation, intelligent learning-based methods have a major role in dynamically modifying communication tactics. To improve reliability, energy efficiency, and overall communication performance in hybrid underwater networks, this paper suggests a learning assisted communication mode selection technique.

Our proposed method is named intelligent underwater wireless communication using Bayesian regularization backpropagation neural network with hybrid optical acoustic transmission (IUWC-BRBNN-HOAT). Our model combines classical machine learning (ML) for rapid mode prediction and Bayesian regularization backpropagation neural network (BRBNN) for deep decision-making. It integrates resource-aware traffic and channel models [4-5], dynamically adapts modulation and coding schemes, to maintain reliable transmission under varying environmental conditions [13], [14], [15]. In our work, the proposed framework is evaluated under analytically modeled underwater channel conditions, providing a controlled feasibility assessment of hybrid opto-acoustic mode selection.

First, we formulate the hybrid optical acoustic mode selection problem as a learning task, under stochastic channel conditions, where the link quality is affected by noise, variability and traffic fluctuations. Conventional ML classifiers perform preliminary link assessment, followed by BRBNN to support robust mode selection under uncertainty. A strict data partitioning strategy is employed to evaluate the performance of training, test and unseen datasets to avoid issues like overfitting.

Results presented in this work demonstrate that the proposed framework achieves improved energy efficiency, throughput, and traffic handling performance compared with existing hybrid underwater communication approaches. The overall paper is structured as follows: Section 2 presents the experimental setup, Section 3 explains the results, and Section 4 provides a conclusion.

Research studies have explored hybrid UWC systems [16], [17] that integrate deep learning with hybrid optical-acoustic transmission techniques [18], [19]. In 2023, Salama, W. M., et al. [20] presented an underwater optical wireless communication system with a deep learning convolutional neural network with non-orthogonal multiple access (UOWC-CNN-NOMA).

In [20], the pairing approach for NOMA nodes was presented. NOMA outperforms the orthogonal multiple access method by about 6% in terms of overall rates. A global optimal power allocation method (GOPA) improves sum rates over fixed power allocation (FPA) and step-by-step sub-optimization algorithm (SSOPA), whereas a SSOPA outperforms FPA.

In 2024, Shin, H., et al. [21] has presented multi-dimensional beam optimization in underwater optical wireless communication based on deep reinforcement learning (MBO-UOWC-DL). Their study suggests adaptive management of optical beam alignment to maintain a seamless connection with good communication performance in a point-to-point (P2P) UOWC. To achieve this, a two-step two-agent deep reinforcement learning (TSTA-DRL) algorithm is used, which allows an underwater sensor (US) installed on the seabed to sequentially determine the beam orientation (BO) and beam divergence (BD) angles before transmitting its sensing data to an unmanned surface vehicle (USV) that may shake irregularly above sea level.

Table 1. Comparison of related works

Ref	Model	Aim	Merits	Demerits
[20]	UOWC-CNN-NOMA	Enhance performance	Boosts throughput	Computational complexity
[21]	MBO-UOWC-DL	Optimize beamforming	Adapts well to dynamic conditions	Requires extensive training time
[22]	ML-UOAC-TI	Improve throughput	Communication flexibility	Depends on channel state information

In 2024, Stewart C., et al. [22] has presented ML depending on underwater optical-acoustic communication channel switching for throughput improvement (ML-UOAC-TI). Their study enhances the reliability and efficiency of UOWC systems by investigating the application of ML approaches for hybrid channel evaluation and transmission decision-making. The primary goal was to enable a UOWC modem to utilize ambient sensor data to predict channel conditions and determine whether to transmit immediately, store data for later transmission, or switch to an alternative communication technique, such as acoustic or radio frequency (RF).

Table 1 presents a summary and comparison of related works. A critical issue to be discussed is survivability in underwater communications, which arises due to the dynamic channel conditions. Two widely used mechanisms for survivability can be stated. Firstly, link-based protection ensures that backup links are available in the event of failure. Secondly, link-based restoration, which is a reactive recovery after failure. In acoustic networks, protection is achieved via multipath and relay-based routing [7-8], [12], while restoration is supported by adaptive re-routing [7], [10]. In optical systems, beam steering and divergence control provide link protection [6], [21]. In Hybrid optical–acoustic systems, survivability is intrinsically improved, as the acoustic link can restore connectivity when the optical link is impaired by turbidity or misalignment [7], [10], [14], [19]. Recent studies highlight ML assisted channel switching as an effective restoration mechanism [11], [14], [22]. These techniques motivate our proposed framework, which integrates neural-network-based switching for resilient hybrid communication.

In their work, Noor et al. outlined a multi-channel hybrid architecture with Tabu search routing algorithm and scheduling the appropriate priority to offer high data rate, but their mode selection used deterministic thresholds, and the strategies to be used for survivability are yet to be addressed [18]. The possibility of acoustic-driven switching is discussed in [19]. The support vector machine (SVM) technique is applied to predict the optical signal-to-noise ratio (SNR) using the acoustic features, but it is limited to providing point forecasts. The works described in [14] and in [16] elaborate a hybrid ML-based mode selection mechanism. The gaps and shortcomings of the above-mentioned are outlined in Table 2.

While all those investigations described in the related works show significant improvement in areas including data throughput, beam optimization, hybrid channel utilization, and long-term communication stability, some technological restrictions remain. These include higher processing intensity, susceptibility to environmental dynamics, synchronization complexity, and greater routing overhead. Such limits highlight the continued challenge of establishing a balanced system that fits both performance and efficiency criteria, particularly under real-time and variable underwater conditions.

IUWC-BRBNN-HOAT addresses these gaps and supports reliable, efficient underwater communication operations [14],[23],[24]. Compared to the shallow ML and deterministic approaches, our proposed system combines heuristic backup resource reserving with BRBNN. Besides, the proposed system facilitates proactive control and risk-aware hybrid switching. To simulate real-world underwater dynamics, a three-type traffic model is considered. Fig. 1 displays a block diagram of the proposed method [14].

2. Experimental setup

Unlike feasibility-oriented learning studies, IUWC-BRBNN-HOAT evaluates learning-assisted mode selection under stochastic channel realizations generated independently for training and testing, avoiding analytical data reuse between evaluation phases [14]. In this simulation, the dataset is created by simulating both acoustic and optical channels alongside realistic traffic patterns for sensor nodes organized into clusters. A cluster represents a geographical region in the ocean, and each cluster has several nodes, such as sensors or AUVs, that communicate locally or forward data to cluster heads using acoustic or optical links. Traffic per node is generated throughout using constant, variable, and bursty patterns, producing a three-dimensional tensor of shape. In three-dimensional spaces, node positions are assigned at random, and distances are calculated for both short-range optical and long-range acoustic transmission.

Table 2. Comparison of the proposed framework with existing approaches

Method	Goal	Mode Selection	Uncertainty Handling	Failure Handling	Optimization Focus
Proposed Work	Intelligent underwater wireless communication with ML-based switching	BRBNN probabilistic prediction	Yes	Predictive and proactive switching	Joint optimization (reliability, BER, energy efficiency)
[14]	Energy-efficient hybrid communication links	BIP-based optimization	No	Not specified	Energy optimization
[16]	Addressing underwater communication challenges	Not specified	Identified as a research gap	Not addressed	Future ML-based optimization
[18]	High-rate hybrid communication system	Deterministic threshold switching	No	Reactive switching	QoS scheduling
[19]	Acoustic-to-optical SNR prediction	SVM-based predictor	No	Prediction only	Performance prediction

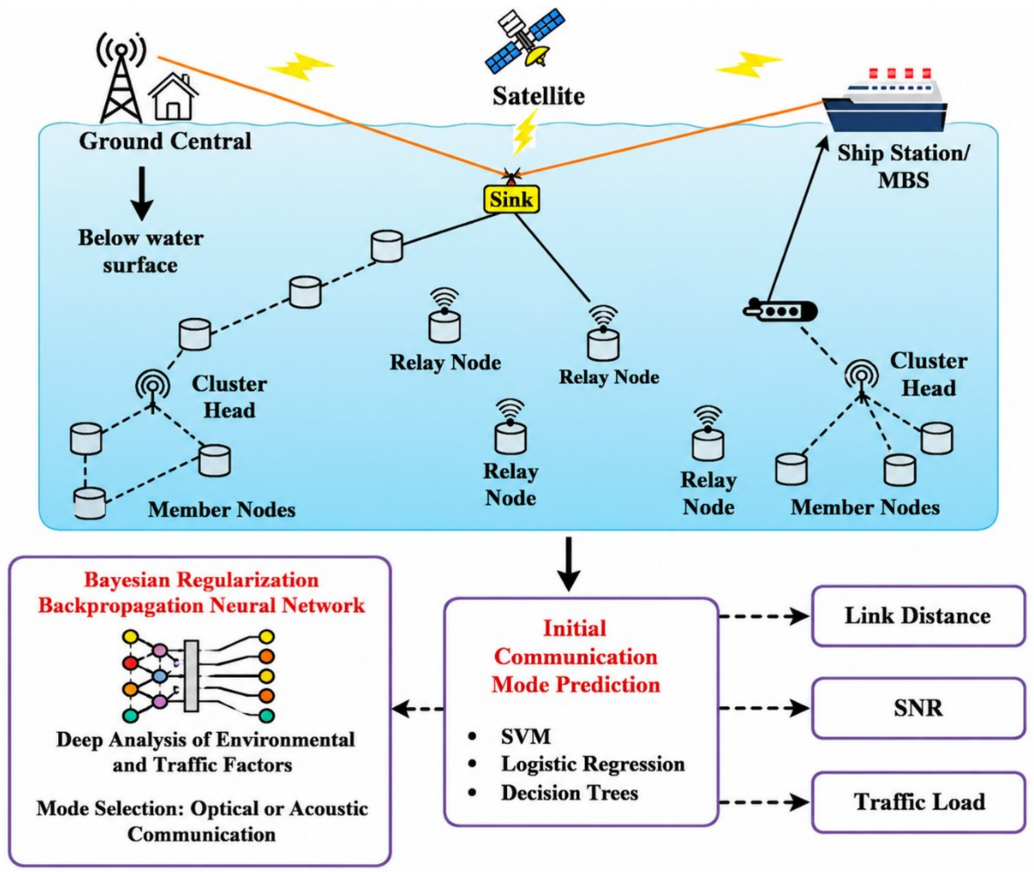

Fig. 1. Block Diagram of the proposed method (colour online)

Channel effects are applied per node each hour, where acoustic and optical attenuation and environmental noise reduce effective throughput and are clipped to non-negative values. Each dataset row comprises timestamp information, cluster and node identifiers, traffic load, effective acoustic and optical throughput, and a label indicating the better communication mode. We have followed the work discussed in [14] to formulate our methodology. The dataset generated in our work includes unique traffic and communication properties for each cluster, allowing for a realistic examination of underwater communication performance across diverse ocean regions. Table 3 shows the summary of the dataset creation steps. Fig. 2 shows the effective acoustic and optical throughput over 7 days for clusters 0, 1, and 2 in the underwater network. Fig. 3(a) depicts the daily average effective throughput for acoustic and optical data. Fig. 3(b) shows the variation of average effective throughput with distance for acoustic and optical data [25]. The presumption of optimum channel conditions allows us to isolate and evaluate the performance gains attributable to the proposed hybrid switching and ML mechanisms.

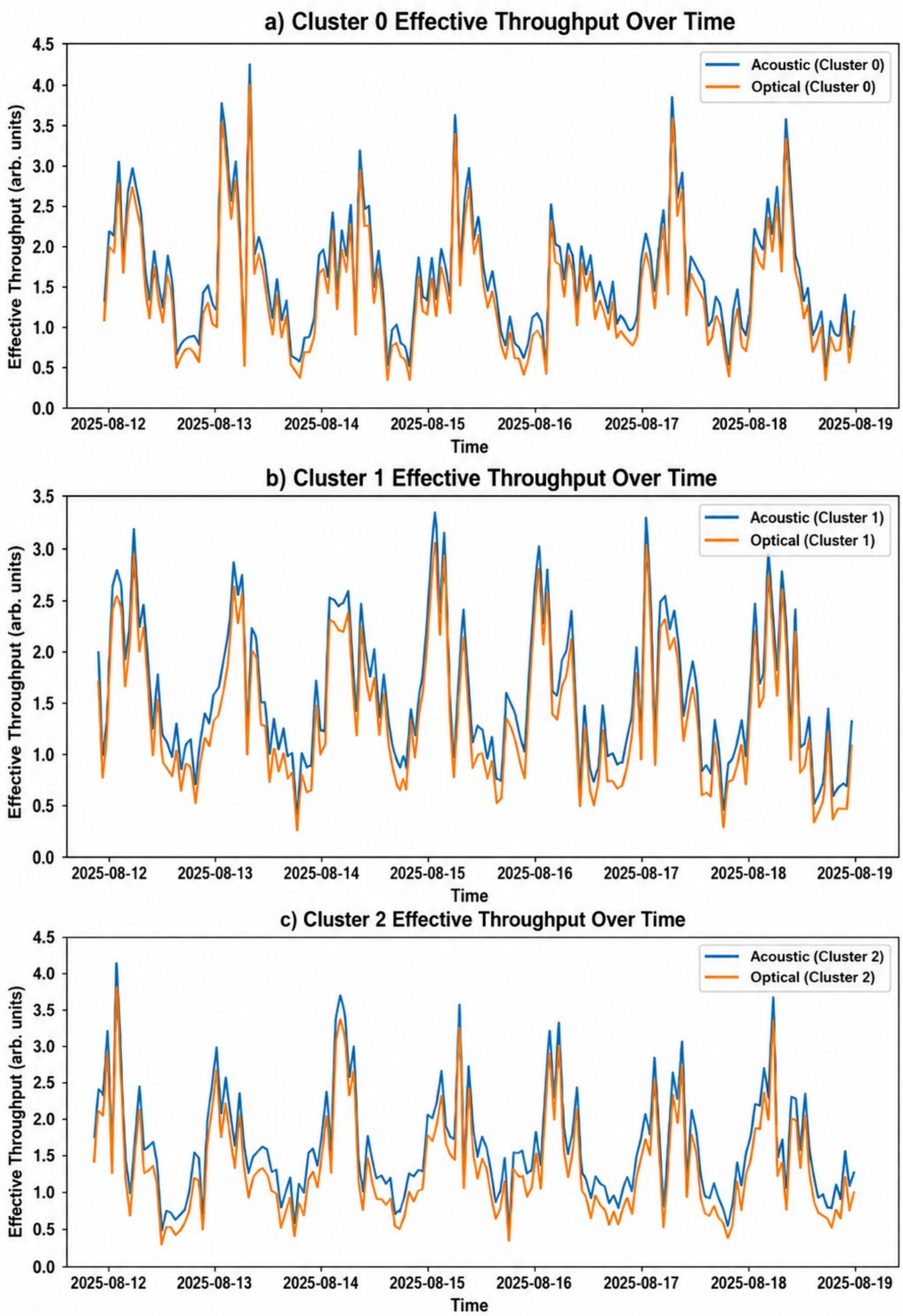

Fig. 2. Effective acoustic and optical throughput over 7 days for a) Cluster 0, b) Cluster 1, c) Cluster 2 (colour online)

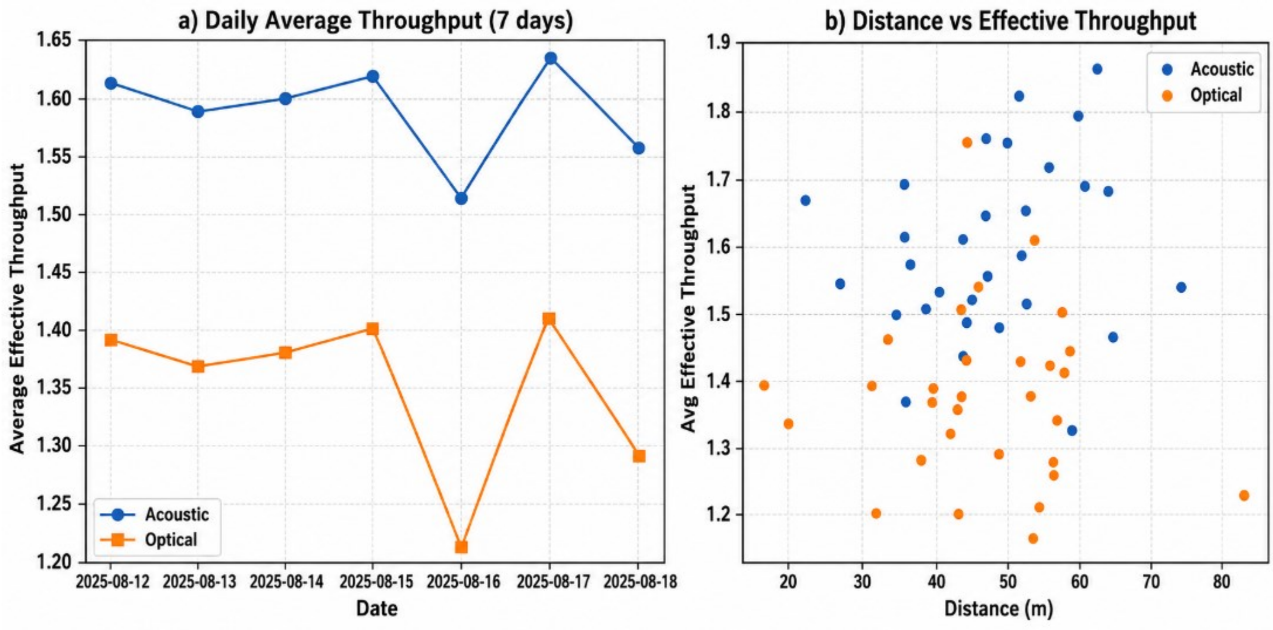

Fig. 3. a) Daily average effective throughput for acoustic and optical data
b) Average effective throughput versus distance for acoustic and optical channels (colour online)

The focus is given to dynamic mode selection based on link distance, traffic load, and environmental SNR without confounding effects from other environmental variables. This approach aligns with prior hybrid system analysis [9], [10], [14], [19], enabling a clear assessment of throughput, energy efficiency, and reliability improvements, which is the primary contribution of this work. Future extensions of our work may incorporate real-time environmental sensing and channel impairments, enabling validation of long-term adaptability and robustness in realistic underwater scenarios. To support accurate prediction and adaptive communication mode selection [26], IUWC-BRBNN-HOAT utilizes seven key input features: d_opt (optimal distance between nodes), d_ac (actual measured distance), L_ac (actual latency observed during transmission), N_ac (actual number of nodes involved in the communication path), L_opt (theoretical optimal latency under ideal conditions), N_opt (ideal number of nodes for efficient transmission), and load (current data traffic or network utilization level). These features capture essential spatial, temporal, and traffic-related dynamics of the underwater environment, enabling classical classifiers to perform effective pre-classification, while the refined data is fed into BRBNN for precise and hybrid communication mode prediction [27].

Conventional mode selection techniques in underwater communications are classified as pre-configured mode selection and pre-calculated mode selection. Pre-configured mode selection based on fixed thresholds defined before deployment appears convenient but is not adaptive in the dynamic underwater conditions. On the other hand, pre-calculated mode selection makes better initial decisions using offline optimization but cannot adjust in varying channel conditions. Therefore, in dynamic underwater environments, neither pre-configured nor pre-calculated approaches guarantee survivability. Our work overcomes these limitations by performing risk-aware selection using BRBNN outputs, allowing proactive failure anticipation and seamless switching.

Classical deep networks may provide only point predictions when confidence is low. As we follow a Bayesian treatment of network weights, enabling uncertainty quantification for failure-tolerant switching, robustness with limited data through priors, and adaptation via probabilistic outputs can be updated. Thus, compared with existing alternatives, BRBNN offers a practical trade-off between computational efficiency and deployment capability in resource-constrained networks.

To enhance decision speed and reduce the load on the BRBNN model, three classical ML approaches, SVM [28], Logistic Regression (LR) [29] and Decision Tree (DT) are used as pre-processing classifiers. These models analyze parameters such as link distance, traffic load, and environmental SNR to predict initial communication modes [30].

First, the initial communication mode is predicted using an SVM approach. SVMs offer high accuracy despite low training data, which is useful in situations where labeled underwater data is scarce. It can adapt to different aquatic environments and properly distinguish communication modes. It reduces the pressure on deeper models such as the BRBNN, resulting in improved overall system efficiency. To choose the best model to start with, a trained SVM categorizes the underwater communication scenario according to link distance, traffic load, and SNR conditions, as provided in equation (1).

$$w^Y y + b = 1, for\ y \in \omega_1 and w^Y y + b = -1, for y \in \omega_2 \quad (1)$$

Here, w is the weight, b represents the bias, y stands for link distance, ω_1 denotes the weight vector normal to the decision hyperplane, ω_2 is the traffic load. The SVM-selected communication mode configures the deep learning module's architecture and feature prioritization paths enabling optimized learning from relevant communication signals. It is given in equation (2).

$$\underset{w,b}{min\,i\,mize}\ \frac{1}{2}\|w\|_2^2 for = 1,\ldots\ldots,z. and y_i(w^Y \Phi y_i b) \geq 1 \quad (2)$$

where, Φ denoted water turbidity, y_i denotes channel stability index.

Table 3. Summary of dataset creation steps for underwater acoustic and optical network simulation

Step	Description	Functions/ Operations	Output
1	Acoustic Channel Model	acoustic_absorption(f_khz)-sound absorption, acoustic_path_loss(d, f_khz) – spreading + absorption loss, acoustic_noise_psd(f_hz) – environmental noise	Acoustic loss and noise per node
2	Optical Channel Model	optical_attenuation(d, kappa) – exponential light attenuation, optical_noise() – Gaussian noise for scattering/turbidity	Optical loss and noise per node
3	Traffic Generator	generate_traffic(num_clusters, nodes_per_cluster, hours) – simulates load: • Constant traffic • Variable (day-night) • Bursty (exponential)	Three-dimensional traffic load
4	Topology (Node Placement)	Random three dimensional coordinates per cluster (np.random.rand(10,3)*100), Distances: dist_opt (node → cluster center), dist_ac (node → network center)	Node positions and distance metrics
5	Channel effects per Node per hour	Compute effective throughput: • eff_ac = load - (L_ac*1e-3 + N_ac*1e-3) • eff_opt = load - (L_opt*1e-2 + N_opt*1e-2) Clip values ≥0	Acoustic and optical effective throughput per node per hour
6	Raw Construction	Include timestamp, topology, traffic load, channel results	Each row represents a node at a given hour
7	Data Frame Assembly	Append all rows into Pandas DataFrame	Final shape = hours ×clusters ×nodes

Next, we used LR to predict the initial communication mode by evaluating the same data parameters. LR is fast and computationally efficient, making it suitable for real-time pre-classification in resource-constrained environments. It is also resistant to mild noise in input features, resulting in consistent predictions under varying underwater conditions. LR models are easy to update, and their linear structure provides rapid convergence, and the effect of each input parameter on the prediction is clearly observable, allowing system designers to fine-tune the mode selection strategy depending on environmental dynamics. Thus, it is given in equation (3)

$$Q(X = 1|X) = \frac{1}{\left(1+r^{-(\beta_0+\beta_1 Y)}\right)} \quad (3)$$

Here, $Q(X = 1|X)$ is the probability of the event $X = 1$ given the predictor variable, β_0 and β_1 are the parameters of the model and r is the base of the natural logarithm.

As a third alternative, we used DT by analyzing the same data parameters. It is suitable for real-time pre-processing in delay-sensitive systems. The DT model is trained using historical or simulated labeled data, splitting nodes based on information gain and assigning terminal labels as optical mode for high-speed short-range or acoustic mode for long-range noise-resilient communication, as given in equation (4).

$$\Omega = \begin{cases} f_{MAX}: [5,7] \\ D_v: [entropy, gini] \end{cases} \quad (4)$$

Here, Ω within which to vary the configuration of the model is defined; D_v and f_{MAX} denotes varying the pair.

To select the best model in the initial communication mode selection process, four performance metrics, accuracy, F1 score, recall, and precision, are used to check which one among SVM, LR and DT is most effective.

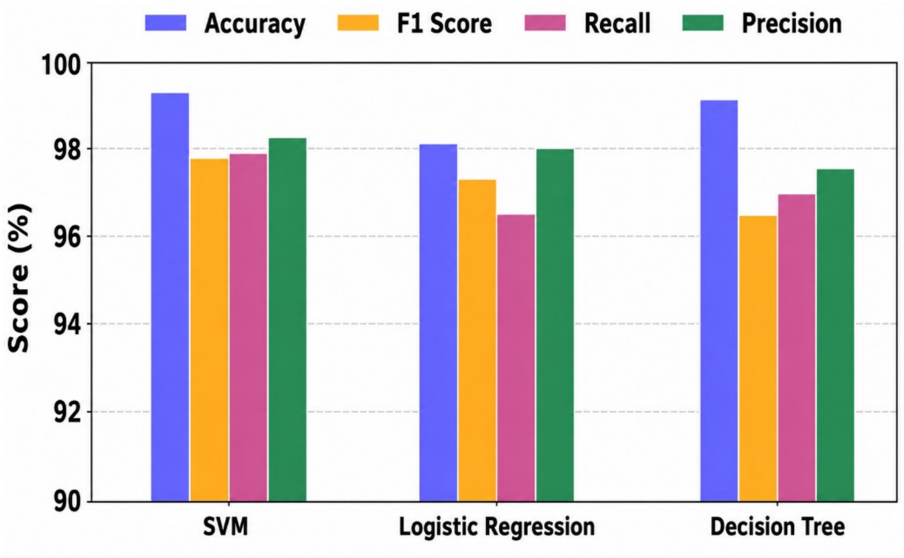

Fig. 4. Performance analysis of initial communication mode prediction models (colour online)

The results, depicted in Fig. 4, highlight that SVM outperformed the other models across all metrics. Based on these results, SVM is selected as the most reliable model for predicting the initial communication mode and this stage operates with relatively low computational complexity and filters communication states before deeper BRBNN processing, thereby helping reduce the effective computational burden and processing overhead.

Table 4. Overview of key parameters and their descriptions for SVM, LR, and DT models

Parameter	**Description**
SVM	
C	Trade-off between correct classification and margin
Gamma	Influences decision boundary smoothness
kernel	Function to project input into higher dimensions
LR	
C	Trade-off between correct classification and margin
penalty	Type of norm used in regularization
solver	Optimization algorithm depending on penalty
max-iter	Ensures convergence
DT	
criterion	Function to measure the quality of a split
max_depth	Controls overfitting
min_sample_split	Avoids splitting small subsets

The refined data, pre-classified by SVM, is then fed into BRBNN for further processing. Table 4 illustrates an overview of all the key parameters and their descriptions for the above three models. The performance variations are addressed by the principles of each classifier. Specifically, grid search cross-validation over the same feature set generated from acoustic-optical channel metrics is used to optimize the models. The final configuration is chosen with maximum classification accuracy and minimum validation loss. Though the models incorporate an identical feature set, it is evident that SVM generalizes smoothly in non-linear decision spaces. The DT model dynamically divides the feature space but is limited to noise susceptibility. Linear dependencies are easily captured by LR models. According to a feature ranking analysis, SVM and DT capitalize on distance and SNR dominating distance limits, whereas in near-linear situations, LR performs effectively.

As mentioned earlier, the initial SVM stage performs lightweight classification, thereby filtering unnecessary samples. This can be quantified by considering the scenario. For an input feature dimension d and n training samples, the computational complexity of the linear SVM classifier is approximately F(nd), whereas the BRBNN stage requires iterative weight updates with higher computational complexity proportional to F(nwh), where w represents the number of trainable weights and h denotes the number of hidden neurons. By activating the BRBNN stage only for selected communication states, the proposed framework significantly reduces redundant neural processing operations.

Generally, BRBNN is used to select a communication model based on complex and dynamic environmental features. It reduces overfitting, resulting in more generalized model performance even with less training data. This leads to improved selection of optimum communication models. Luu et al., in their work, mentioned that when trained on sparse or noisy data, BRBNN maintains high classification accuracy and provides better-calibrated decisions than traditional backpropagation neural network (BPNN), which only provides point estimates of the weights and frequently produces overconfident predictions [31,32].

The communication data is labeled using acoustic and optical modes. The most efficient model is chosen based on the recorded ambient variables, as indicated by equation (5).

$$F = \{(v_1, y_{o1}), (v_2, y_{o2}), \dots., (v_{nt}, t_{ont})\} \qquad (5)$$

Here, F is the input feature matrix, v_1 denotes target output vector, y_{o1} represents the bias matrix of the neural network, v_{nt} denotes the total number of layers, t_{ont} implies the number of training samples. Setting up a BRBNN with input nodes for environmental variables, optimized hidden layers, neurons, and an output layer that classifies communication model types is represented by equation (6).

$$G(\bar{e}) = \text{ɯ}\bar{e}^T\bar{e} + vR_D = \text{ɯ}R_w + vR_D \qquad (6)$$

Here, G denotes reduced weight size in network errors cost, ɯ implies regularization parameter, R_w signifies the sum of squared network weights, $(\bar{e})$ implies a vector of size, v represents the shipping activity factor and R_D denotes an acoustic receiver with a narrow bandwidth. In BRBNN, regularization is embedded in the prior distribution of the weights. The regularization coefficient λ is a regularization parameter that penalizes large weights in the cost function, balancing data-fitting accuracy with model complexity. Physically, it controls the bias–variance trade-off. A high value of λ means smoother models.

Training the network using backpropagation with Bayesian regularization to minimize prediction error and complexity, automatically preventing overfitting by penalizing large weights, is given in equation (7).

$$Q(F|\bar{e}, v, Z_N) = \frac{exp(-vR_D)}{M_F(v)} \qquad (7)$$

where, Q denotes learning rate, F represents the downwelling spectral irradiance and Z_N represents includes both data and regularization gradients and $M_F(v)$ is the effective number of parameters. Input environmental data into the trained BRBNN to predict the most suitable communication model based on learned environmental conditions is given in equation (8).

$$\gamma = L - \text{ű} * tr(J *)^{-1} \qquad (8)$$

Here, γ denotes count of effective parameter exhausted in decreasing error function, ű implies assumed uniform prior density, and $J *$ represents the Hessian matrix of the objective function assessed. The network is periodically retrained with new data to ensure continuous adaptability as represented in equation (9).

$$J^* \approx K^T K \qquad (9)$$

where, K signifies a Jacobean matrix created using the initial derivatives of network error with network weight and T is the Earth's blackbody temperature. Table 5 shows the layer parameter settings of the BRBNN model.

Table 5. BRBNN layer parameter settings

Parameter	Values
units	64
activation	relu
kernel_regularizer (L2 λ)	0.1
dropout rate	0.5

Once the BRBNN has selected the communication mode, the proposed system activates the appropriate modulation and coding combination. The fundamental novelty of IUWC-BRBNN-HOAT is hybrid mode selection and dynamic switching between optical and acoustic communication modes. To support this adaptive behavior, appropriate modulation and error correction techniques are used for each communication medium. This context-aware modulation and coding strategy enables the system to maintain reliable, energy-efficient communication across varying underwater conditions. By this, the proposed framework ensures sustained throughput and communication quality in both short-range optical and long-range acoustic scenarios.

Table 6. Refined simulation parameters

Parameter	Description	Typical Range	Unit
dist	Transmission distance for signal propagation	1 – 1000	meters (m)
freq_khz	Acoustic frequency used for path loss calculation	10 – 100	KiloHertz (kHz)
freq_hz	Frequency input for acoustic noise PSD	100 – 100000	Hertz (Hz)
alpha	Acoustic absorption coefficient	0.1 – 10	decibels/km (dB/km)
extinction_coeff	Optical extinction coefficient	0.05 – 0.5	1/meters (1/m)
L_ac	Acoustic path loss	20 – 150	decibels (dB)
N_ac	Acoustic noise PSD	30 – 100	dB re μPa²/Hz
L_opt	Optical attenuation	1 – 20	decibels (dB)
N_opt	Total optical noise power	1e-14 – 1e-11	Watts (W)
thermal_noise	Thermal noise power in optical systems	1e-13 – 1e-12	Watts (W)
dark_current	Dark current noise in optical receivers	1e-13 – 1e-12	Watts (W)
shot_noise	Quantum shot noise	1e-15 – 1e-13	Watts (W)
ambient_noise	Ambient light noise	1e-13 – 1e-12	Watts (W)
Nt	Turbulence noise spectral density	20 – 60	dB re μPa²/Hz
Ns	Shipping noise spectral density	40 – 80	dB re μPa²/Hz
Nw	Wave noise spectral density	50 – 90	dB re μPa²/Hz
Nth	Thermal noise spectral density (acoustic)	10 – 50	dB re μPa²/Hz
snr_db	Signal-to-Noise Ratio	5 – 30	decibels (dB)
snr_linear	Linear SNR	3 – 1000	unitless
ber	Bit Error Rate	0 – 0.1	unitless
SIM_DURATION	Total simulation time	10 – 1000	seconds (s)
PKT_SIZE_BITS	Packet size	800 – 10000	bits
AC_DATA_RATE	Acoustic channel data rate	1000 – 10000	bps
OP_DATA_RATE	Optical channel data rate	1e6 – 1e9	bps
P_AC	Acoustic power per transmission	0.5 – 5.0	Watts (W)
P_OP	Optical power per transmission	0.05 – 1.0	Watts (W)
AC_DROP_PROB	Packet drop probability (acoustic)	0 – 0.2	unitless
OP_DROP_PROB	Packet drop probability (optical)	0 – 0.2	unitless
acoustic_pdr	Packet Delivery Ratio (acoustic)	0.8 – 1.0	unitless
optical_pdr	Packet Delivery Ratio (optical)	0.8 – 1.0	unitless
acoustic_avg_delay_s	Average delay per acoustic packet	0.01 – 0.5	seconds (s)
optical_avg_delay_s	Average delay per optical packet	0.001 – 0.05	seconds (s)
actual_energy_J	Total hybrid switching energy	1 – 50	Joules (J)
baseline_energy_J	Energy if acoustic only used	2 – 100	Joules (J)
energy_saved_J	Energy saved due to ML switching	0 – 50	Joules (J)
avg_pwr_savings_W	Average power saved	0 – 1	Watts (W)
load	Traffic load per node	0 – 1e6	bits/sec
acoustic_recv_bps	Acoustic received throughput	0 – 10000	bps
optical_recv_bps	Optical received throughput	0 – 1e8	bps
acoustic_offered_bps	Acoustic offered load	0 – 10000	bps
optical_offered_bps	Optical offered load	0 – 1e8	bps
acoustic_norm_load	Normalized acoustic load	0 – 1	unitless
optical_norm_load	Normalized optical load	0 – 1	unitless

3. Results and discussion

Table 6 shows the refined simulation parameters. When we have examined how the loss function changes during the BRBNN training process, we have observed that the training and validation loss decrease dramatically in the initial phase, epochs 0-10, indicating rapid learning. The training loss drops from roughly 5.0 to 0.5 and the validation loss follows a similar path, indicating effective learning and generalization. Further, the pace of decline slows, but both losses continue to fall, indicating that the model is stabilizing. By epochs 40-100, the loss values have plateaued.

Also, we have checked the model's accuracy during training. The training accuracy and validation accuracy rise in the early epochs, indicating that the model rapidly improves its ability to generate the right predictions. By epoch 5, the accuracy of both the training and validation sets shows rapid learning. The constant overlap of the training and validation accuracy curves has indicated that the model is effectively generalizing without overfitting and performing remarkably well on both seen and unseen data. Thus, it has been observed that the BRBNN model has successfully learned the underlying data patterns and applied them to new, previously unknown data.

By treating the network weights as random variables and penalizing large weights in the loss function, BRBNN automatically controls model complexity and reduces overfitting, making it especially beneficial when the dataset is small or noisy when compared to standard

BPNN. Previous comparative studies have shown that BRBNN generally achieves lower generalization error and more stable performance, particularly in regression problems with nonlinear, noisy data, while requiring no separate validation set for early stopping.

BRBNN offers an estimate of predictive uncertainty via the posterior distribution over weights, enabling confidence information in addition to point predictions, which is essential for underwater communication tasks that depend on safety or dependability. Using the same dataset, we made a brief comparison between the suggested BRBNN and a simple BP network. The standard back propagation (BP) model used for comparison is a classical feedforward neural network trained with ordinary gradient descent backpropagation (non-Bayesian). With a smoother validation loss curve shown in Fig. 5 and a marginally higher test accuracy, BRBNN demonstrated better generalization and less overfitting under noisy, heterogeneous inputs.

Additionally, Fig. 6 shows the predicted mean with an approximate 95% confidence interval, demonstrating its capacity to convey predictive uncertainty. When we additionally test the trained model on an unseen dataset created under various random seeds and traffic realizations, it has been observed that novel environmental and traffic conditions have not been encountered during training. This unknown dataset simulates deployment-time uncertainty by including differences in traffic load distributions. For the training set, test set, and unseen dataset, performance measures are observed. Strong generalization and robustness are confirmed by the results, which show that the IUWC-BRBNN-HOAT framework maintains constant performance across those datasets with very slight degradation on unseen data.

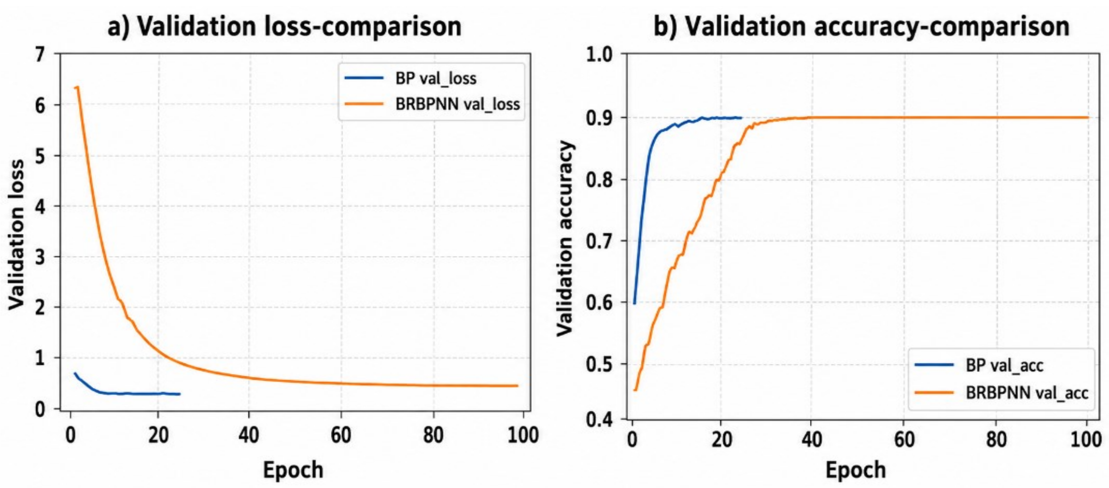

Fig. 5. a) Validation loss of plain BP and BRBNN networks over training epochs b) Validation accuracy of plain BP and BRBNN networks over training epochs (colour online)

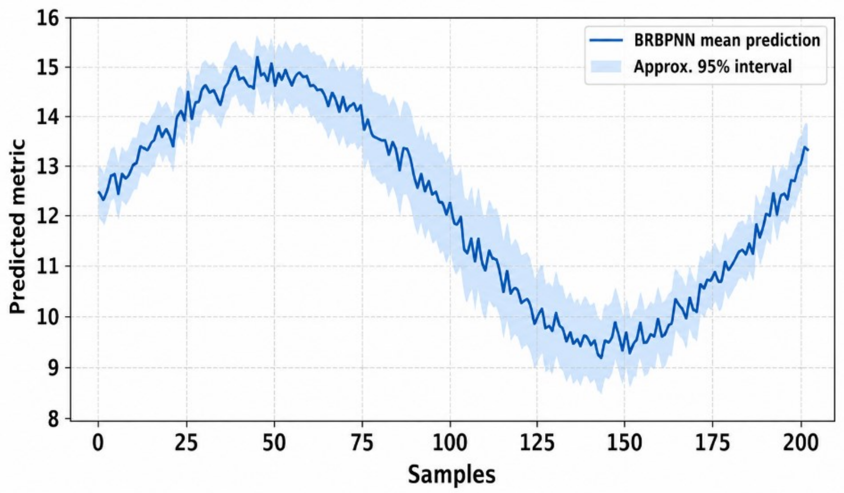

Fig. 6. Illustration of BRBNN predictive uncertainty with mean (colour online)

Fig. 7 portrays the simulation results of the proposed method, analyzed with UOWC-CNN-NOMA [20], MBO-UOWC-DL [21] and ML-UOAC-TI [22] models, respectively. All three comparison methods were simulated under identical conditions. This ensures a fair comparison across all metrics. Fig. 7(a) depicts energy consumption in achieving desired outcomes. The proposed model achieves up to 75% lower energy consumption compared to baseline models, making it highly suitable for energy-constrained IoUT networks. Fig. 7(b) illustrates the IUWC-BRBNN-HOAT model throughput in achieving desired outcomes. Our model achieves the highest throughput throughout the range, starting at 15.41 kbps at 0 m and peaking at 29.04 kbps at 8 m, with a slight drop to 28.50 kbps at 10 m. In comparison, UOWC-CNN-NOMA ranges from 5.19 kbps to 14.54 kbps, MBO-UOWC-DL grows from 1.97 kbps to 14.66 kbps, and ML-UOAC-TI remains relatively stable between 10.55 kbps and 14.19 kbps.

From Table 7, it is evident that the inclusion of the lightweight SVM pre-classification stage reduces the average processing time compared with other methods. This reduction is particularly beneficial for resource-constrained underwater nodes, where computational power and battery availability are limited.

Table 7. Computational comparison of different learning approaches

Method	Average processing time(ms)	Relative computational complexity
UOWC-CNN-NOMA[20]	12.8	high
MBO-UOWC-DL[21]	10.6	high
ML-UOAC-TI [22]	8.9	moderate
Proposed method	5.2	Low to moderate

The higher performance is due to the learning-assisted communication mode selection employing BRBNN and hybrid optical-acoustic transmission. We thus conclude that the performance of the IUWC-BRBNN-HOAT method provides 27.52 % lower energy consumption and 15.41 % higher throughput compared to existing approaches described in [20],[21], and [22], under identical simulation conditions.

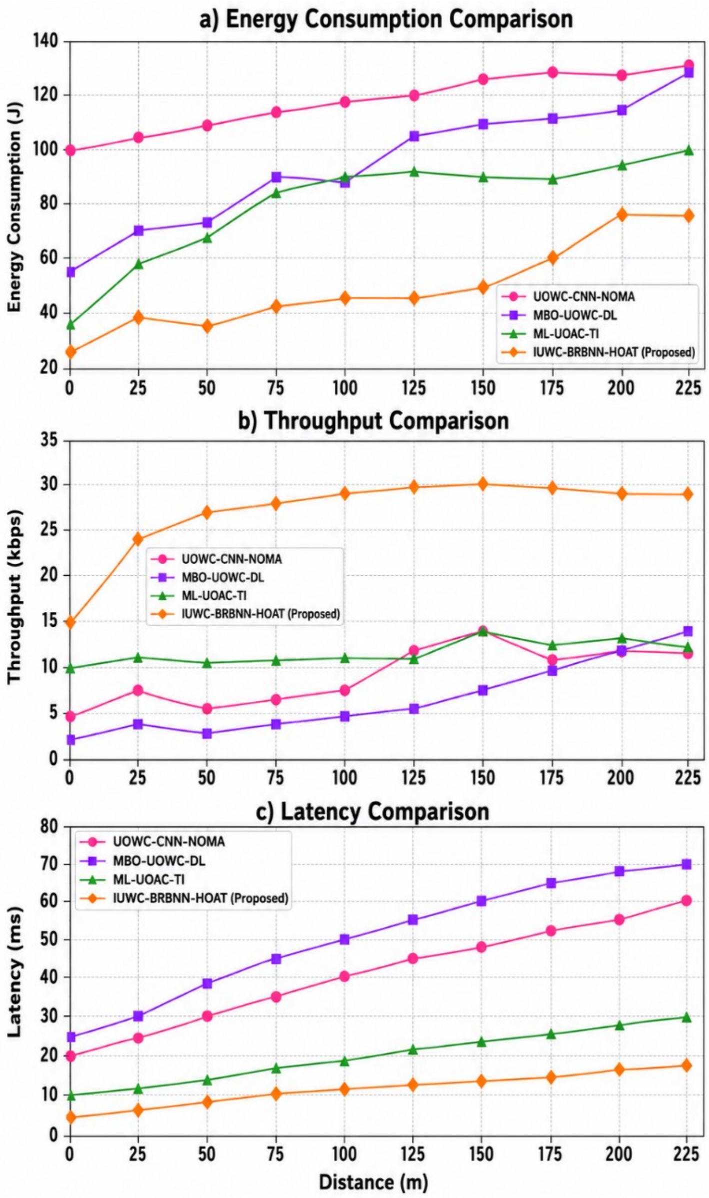

Fig. 7. Performance analysis of a) Energy Consumption b) Throughput c) Latency (colour online)

4. Conclusions

This study successfully demonstrates the implementation of the IUWC-BRBNN-HOAT framework, which employs a learning-assisted mode selection for hybrid optical–acoustic UWC under stochastic channel conditions, for improved IoUT communication. On investigating classical ML models for initial mode prediction, the SVM-based pre-classifier proves to be the most stable and reliable model. BRBNN further enhances decision robustness. The proposed method achieves a higher received load compared with existing methods for the generated scenario. Simulations performed in our work confirm that the proposed approach improves mode selection robustness under dynamic environments. Future work will focus on integrating real-time environmental sensing hardware and deploying a framework in live underwater testbeds to assess long-term adaptability and robustness. Also, we plan to incorporate richer stochastic traffic and channel variations to enable a more detailed statistical analysis with non-negligible standard deviations. Comparative analysis with other hybrid protocols with real-time data will further validate its practicability for large-scale oceanic applications.

References

[1] M. C. Domingo, J. Netw. Comput. Appl. **35**(6), 1879 (2012).
[2] S. A. H. Mohsan, A. Mazinani, N. Q. H. Othman, H. Amjad, Earth Sci. Inform. **15**(2), 735 (2022).
[3] O. Bello, S. Zeadally, Ad Hoc Netw. **135**, 102933 (2022).
[4] K. Y. Islam, I. Ahmad, Y. Rong, D. Habibi, IEEE Internet of Things Journal **11**(8), 14282 (2024).
[5] W. Pu, W. Zhu, Y. Qiu, IEEE Sens. J. **24**(16), 26731 (2024).
[6] H. Shin, S. M. Kim, Y. Song, IEEE Internet of Things Journal **10**(24), 22726 (2023).
[7] H. M. Oubei, Chao Shen, Abla Kammoun, Emna Zedini, Ki-Hong Park, Xiaobin Sun, Guangyu Liu, Chun Hong Kang, Tien Khee Ng, Mohamed-Slim Alouini, Boon S. Ooi, Jpn. J. Appl. Phys. **57**(8), 08PA06 (2018).
[8] C. Wang, X. Shen, H. Wang, H. Zhang, H. Mei, IEEE Sens. J. **23**(15), 17771 (2023).
[9] C. Wang, X. Shen, H. Wang, W. Xie, H. Mei, H. Zhang, IEEE Sens. J. **24**(7), 11562 (2024).
[10] D. Zhang, I. N'doye, T. Ballal, T. Y. Al-Naffouri, M. S. Alouini, T. M. Laleg-Kirti, IEEE Internet of Things Journal **7**(10), 10048 (2020).
[11] H. Luo, Z. Xu, J. Wang, Y. Yang, R. Ruby, K. Wu, Wirel. Commun. Mob. Com. **2022**, 9471698 (2022).
[12] R. Diamant, P. Casari, F. Campagnaro, O. Kebkal, V. Kebkal, M. Zorzi, IEEE T. Wirel. Commun. **17**(3), 1738 (2018).
[13] J. Cao, J. Dou, L. Chu, C. Qu, L. Wang, B. Zhao, IEEE Commun. Lett. **26**(4), 788 (2022).
[14] K. Y. Islam, I. Ahmad, D. Habibi, M. I. A. Zahed, J. Kamruzzaman, IEEE Access **9**, 85109 (2021).
[15] F. Yu, F. Xiao, C. Li, E. Cheng, F. Yuan, IEEE J. Oceanic Eng. **50**(2), 919 (2025).
[16] T. Theocharidis, E. Kavallieratou, Telecommun. Syst. **88**(2), 201 (2025).
[17] J. I. D. O. Filho, A. Trichili, B. S. Ooi, M. S. Alouini, K. N. Salama, IEEE Commun. Mag. **58**(1), 68 (2020).
[18] K. Noor, H. Shahid, H. M. Obaid, A. Rauf, A. Yousaf, A. Shahid, Wireless Pers. Commun. **125**(3), 2219 (2022).
[19] R. Diamant, F. Campagnaro, M. de Fillipo de Grazia, P. Casari, A. Testolin, V. S. Calzado, IEEE T. Wirel. Commun. **16**(12), 8037 (2017).
[20] W. M. Salama, M. H. Aly, E. S. Amer, Opt. Quant. Electron. **55**(5), 467 (2023).
[21] H. Shin, S. Baek, Y. Song, IEEE Internet of Things Journal **11**(17), 28623 (2024).
[22] C. Stewart, A. Muhammad, W. K. Fung, N. Fough, R. Prabhu, Proc. IEEE MetroSea **2024**, 46 (2024).
[23] P. A. Hoeher, J. Sticklus, A. Harlakin, IEEE Commun. Surv. Tut. **23**(4), 2630 (2021).
[24] J. Xu, Y. Zhang, J. Lightwave Technol. **43**(4), 1644 (2025).
[25] T. Qiu, Z. Zhao, T. Zhang, C. Chen, C. L. P. Chen, IEEE T. Ind. Inform. **16**(7), 4297 (2020).
[26] S. Han, Y. Noh, R. Liang, R. Chen, Y. J. Cheng, M. Gerla, China Commun. **11**(5), 49 (2014).
[27] X. Zhao, Z. Qi, D. Pompili, Comput. Netw. **242**, 110233 (2024).
[28] J. S. Pimentel, R. Ospina, A. Ara, Decision Analytivs Journal **11**, 100457 (2024).
[29] B. Kolukisa, B. K. Dedeturk, H. Hacilar, V. C. Gungor, Computer Standards & Interfaces **89**, 103808 (2024).
[30] X. Hou, J. Wang, Z. Fang, X. Zhang, S. Song, X. Zhang, Y. Ren, IEEE Network **35**(4), 160 (2021).
[31] S. Gouravaraju, J. Narayan, R. A. Sauer, S. S. Gautam, J. Adhesion **98**(12), 1714 (2022).
[32] V. C. Luu, J. Park, J. P. Hong, IEEE Internet of Things Journal **11**(13), 24300 (2024).

*Corresponding author: asangeetha@vit.ac.in